THE JOURNAL OF PHYSICAL CHEMISTRY A

Article

pubs.acs.org/JPCA

X-ray Absorption Spectroscopy of Ground and Excited Rhenium–Carbonyl–Diimine Complexes: Evidence for a Two-Center Electron Transfer

A. El Nahhas,[†,¶] R. M. van der Veen,[†,#] T. J. Penfold,[†,‡,§] V. T. Pham,[†,@] F. A. Lima,[†,△] R. Abela,[§] A. M. Blanco-Rodriguez,[⊥] S. Záliš,[∥] A. Vlček,*[,∥,⊥] I. Tavernelli,[‡] U. Rothlisberger,[‡] C. J. Milne,[†,▽] and M. Chergui*[,†]

[†]École Polytechnique Fédérale de Lausanne, Laboratoire de spectroscopie ultrarapide, ISIC, FSB-BSP, CH-1015 Lausanne, Switzerland

[‡]École Polytechnique Fédérale de Lausanne, Laboratoire de chimie et biochimie computationnelles, ISIC, FSB-BSP, CH-1015 Lausanne, Switzerland

[§]SwissFEL, Paul Scherrer Institute, CH-5232 Villigen, Switzerland

[∥]J. Heyrovský Institute of Physical Chemistry, Academy of Sciences of the Czech Republic, Dolejškova 3, Prague, Czech Republic

[⊥]School of Biological and Chemical Sciences, Queen Mary University of London, Mile End Road, London E1 4NS, U.K.

Supporting Information

ABSTRACT: Steady-state and picosecond time-resolved X-ray absorption spectroscopy is used to study the ground and lowest triplet states of $[ReX(CO)_3(bpy)]^{n+}$, X = Etpy (n = 1), Cl, or Br (n = 0). We demonstrate that the transient spectra at both the Re L_3- and Br K-edges show the emergence of a pre-edge feature, absent in the ground-state spectrum, which is associated with the electron hole created in the highest occupied molecular orbital following photoexcitation. Importantly, these features have the same dynamics, confirming previous predictions that the low-lying excited states of these complexes involve a two-center charge transfer from both the Re and the ligand, X. We also demonstrate that the DFT optimized ground and excited structures allow us to reproduce the experimental XANES and EXAFS spectra. The ground-state structural refinement shows that the Br atom contributes very little to the latter, whereas the Re–C–O scattering paths are dominant due to the so-called focusing effect. For the excited-state spectrum, the Re–X bond undergoes one of the largest changes but still remains a weak contribution to the photoinduced changes of the EXAFS spectrum.

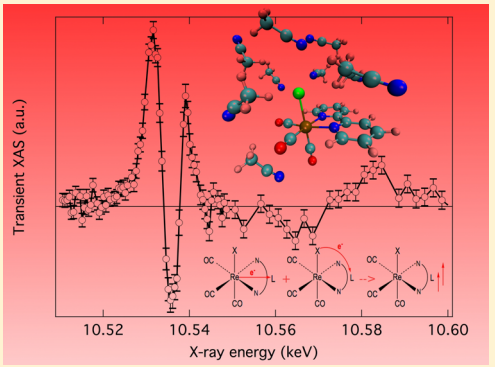

INTRODUCTION

Understanding the structure and bonding of metal diimine complexes is a challenging problem, with implications to the description of their electronic structure, namely the role of the metal d-orbitals and the metal–ligand π bonding. The $[ReX(CO)_3(bpy)]^{n+}$ (X = halide or pseudohalide, bpy = 2,2′-bipyridine or analogous α-diimines, Figure 1) complexes, which are of interest here, are notable examples of metal complexes that exhibit a highly mixed and complex electronic structure. In particular, their valence space is composed of a π-electron donating halide (or pseudohalide) with π-electron accepting CO and bpy ligands. The Re atom is in a +1 oxidation state and has a $5d^6$ electron configuration with all three dπ orbitals occupied. The highest occupied molecular orbitals (HOMOs) consist of two pairs of Re–X π-bonding and antibonding MOs arising from the interaction between two of the halide valence p-orbitals with the corresponding Re 5dπ orbitals. CO and, to a lesser extent, the bpy orbitals also contribute to high-lying MOs because of π back-bonding. Density functional theory (DFT)[1,2] showed that the Re halogen moiety is strongly mixed in the HOMO and HOMO−1 orbitals: the dπ(Re) contribution to these orbitals is ∼53% and ∼47% when X = Cl or Br, respectively, whereas the corresponding pπ(halide) contribution is ∼18% (Cl) and ∼26% (Br). In contrast, for X = Etpy, the HOMO and HOMO−1 are predominantly (60–66%) dπ(Re), mixed with π^*(CO).[2]

The lowest unoccupied orbitals, which are of importance for the population of long-lived and inherently stable charge-transfer (CT) states under near-UV or visible irradiation, consist of several predominantly (at least 90%) π^*(bpy) and, higher in energy, π^*(CO) levels. Therefore, the low-lying excited states for these complexes are expected to exhibit a Re

Received: October 27, 2012
Revised: December 11, 2012
Published: December 18, 2012

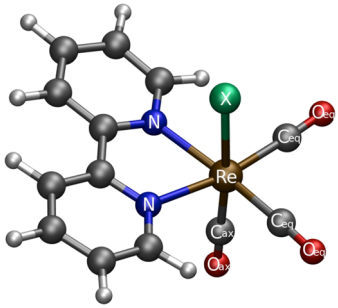

Figure 1. Schematic structure of $[ReX(CO)_3(bpy)]^{n+}$, X = Cl, Br (n = 0) or Etpy (n = 1).

→ bpy and X → bpy CT character,[1,3−5] due to the strongly mixed metal−halogen moiety of the HOMO, and this has led them to being labeled as metal−ligand-to-ligand charge-transfer (MLLCT) states. However, direct experimental evidence of this two-center transfer has been so far lacking. The first indication of an MLLCT was provided by the resonance Raman spectrum of $[ReBr(CO)_3(N,N'$-bis-p-tolyl-1,4-diazabutadiene)] that shows enhancement of the band due to the Re−Br stretching vibration, when excited at the Re diazabutadiene MLCT transition.[6] Later, picosecond IR studies of $[Re(NCS)(CO)_3(N,N'$-bis-p-tolyl-1,4-diazabutadiene)], where the NCS^- ligand is a π-donating pseudohalide, showed that the ν(CO) vibrational bands of the $Re(CO)_3$ moiety shifts to higher energies upon excitation, while the ν(NC) band of the NCS^- ligand shifts to lower ones. These spectral shifts were attributed to a partial depopulation of π^*(CO) and $\pi(NCS^-)$ orbitals, pointing to the MLCT and LLCT contributions to the lowest (triplet) excited state, respectively, in accord with the DFT calculated electron-density redistribution.[7]

Although these results, along with theory, provide strong support in favor of the MLLCT character of the excited state, the most direct way to visualize the change of oxidation state of atomic species within a photoexcited molecule is time-resolved X-ray absorption spectroscopy (XAS). Here, edge shifts and the appearance of new pre-edge transitions point to changes of the oxidation state and atomic/molecular orbital character and occupancy.[8−10] In addition, the above-ionization XANES (X-ray absorption near-edge structure) and EXAFS (extended X-ray absorption fine structure) regions of the spectrum contain information about the molecular structure around the absorbing atom. Differences in the XANES and EXAFS regions after excitation reflect structural changes in the excited state of the molecule and eventually, also, in its solvation shell. These capabilities of XAS have been exploited to probe photoinduced oxidation-state change and the accompanying structure of a number of metal complexes in solution[8−11] and of iodide in water.[12] Because of its ability to interrogate different atoms in the molecule, time-resolved XAS is ideal for addressing the question of the MLCT/LLCT excited-state character of halogenated Recarbonyl complexes, by probing the photo-induced changes at the Re L_3-edge and the halogen K-edge.

Only a few XAS studies of ground-state Re complexes have so far been reported.[13−17] Interestingly, several features of their L_3-edge spectra resemble, to some extent, those reported here. Sarode[13] presented the spectrum of Re in cesium hexachlororhenate(IV) showing a main peak due to the white line, typical of the L-edge spectra of transition metals.[18] The spectrum also exhibited a shoulder in the pre-edge region, which was assigned to transitions into the Re 5d(t_{2g}), as Re^{4+} has three vacancies in the d(t_{2g}) orbitals of this octahedral complex. Later, Sham et al.[16] and Kuzmin et al.[15,17] reported the Re L_3-edge for $Re_2(CO)_{10}$ and ReO_3, respectively. Their spectra lack the pre-edge feature due to the oxidation state of the metal, but they both exhibit the white line and a feature just above it, for which no interpretation was given. Finally, Popov et al.[19] reported spectra for the Re $L_{2,3}$-edges of double perovskites with the d-occupancy of Re varying from 0 to 5. In none of these cases was a pre-edge feature reported, but the white line exhibited a clear doublet structure, separated by ∼3 eV, whose intensity was reversed between the L_2- and L_3-edges. Finally, several authors have reported XAS studies of Re catalysts supported on metal oxides (see refs 14 and 20 and references therein). In these cases, the spectra were mostly used to represent trends as a function of temperature and reducing agent. Nevertheless, Bare et al.[14] used the FEFF code[21] to simulate changes in the XANES spectrum as a function of Re cluster size for both free and supported clusters. They concluded that a reduction of the white line intensity with the size of the clusters was due to its interaction with the aluminum surface, which caused a broadening of the density of states (DOS), reflecting a reduction in symmetry. This is further evidenced by Hilbrig et al.[20] who also studied Re deposited on Al_2O_3 surfaces and demonstrated a significant reduction of the intensity of the white line feature between solid state and aqueous NH_3ReO_4 solution, which they tentatively assigned to a distinct and different band structure between the two systems as a result of the different second neighbor ligands.

In this contribution, we present and discuss the Re L_3-edge (i.e., transitions from the $2p_{3/2}$ core orbital) of three ground-state $[ReX(CO)_3(bpy)]^{n+}$ complexes, where X = Cl, Br (n = 0), and Etpy (n = 1), and for X = Br, the Br K-edge spectrum in two different solvents. We extract the structure of the complex from the EXAFS spectrum, which is found to be in good agreement with the DFT calculations.[2,22] Using multiple scattering (MS) theory implemented in the FDMNES package,[23] we show that the white line arises from transitions into the empty Re 5d orbitals, but that they are somewhat modulated by the ligand structure. We will also present the Br K-edge XANES spectrum to stress the importance of solvent effects, which we discuss in terms of quantum mechanics/molecular mechanics (QM/MM)[24−26] molecular dynamics (MD) simulations. Finally, we will present picosecond XAS transients of the Etpy, Br, and Cl containing complexes. For X = Br, they unambiguously identify for the first time the MLLCT character of the excited triplet state in such complexes, whereas analysis of the transient EXAFS spectrum allows us to extract the excited-state structure, in good agreement with the DFT calculations.

RESULTS

The experimental procedure for the static and the picosecond XAS experiments has already been described in refs 11 and 27 and is presented along with the theoretical methodology in the Supporting Information.

Steady-State Spectra. Figure 2 shows the ground-state Re L_3-edge absorption spectrum of 100 mM solution of $[ReX(CO)_3(bpy)]^{n+}$ in N,N-dimethylformamide, recorded in transmission mode. The inset zooms into the XANES region and highlights, somewhat surprisingly, that the spectra are rather insensitive to the X ligand. Several features appear in all spectra: (i) A weak pre-edge feature (labeled A), (ii) a more intense

dx.doi.org/10.1021/jp3106502 | J. Phys. Chem. A 2013, 117, 361−369

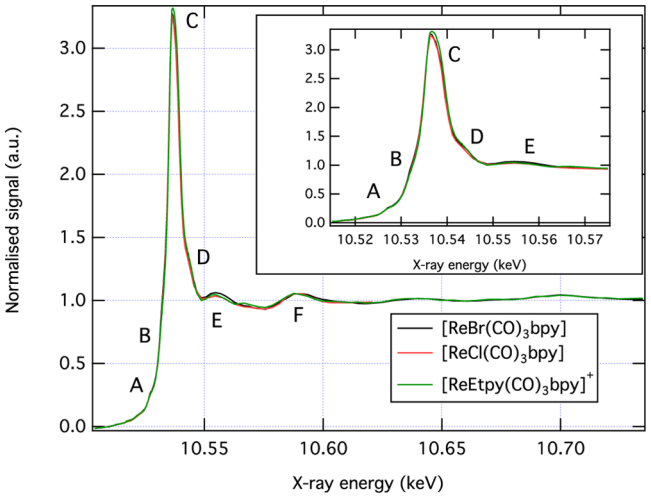

Figure 2. Normalized Re L_3-edge spectrum for $[ReBr(CO)_3(bpy)]$ (black), $[ReCl(CO)_3(bpy)]$ (red), and $[ReEtpy(CO)_3(bpy)]^+$ (green). Inset: enlargement of the XANES region of the spectrum.

pre-edge feature (labeled B) at ~10.532 keV, (iii) the white-line (labeled C) with a shoulder on the high-energy side, and (iv) the above ionization resonances D and E.

The asymmetric profile of the white line (C), which is suggestive of a doublet structure, is reminiscent of the observations on double perovskites, which were attributed to the ligand field splitting (~3 eV) of the d-orbitals into t_{2g} and e_g orbitals,[19] except that in this case the shoulder is on the low-energy side. The L_3-edge spectrum presented by Sarode for $CsReCl_6$[13] also bears some resemblances with that of Figure 2, with the pre-edge B feature and the white line (C), although it is not clear if the latter has a doublet structure. He attributed the pre-edge feature to a $2p_{3/2} \rightarrow t_{2g}$ transition, whereas the white line was attributed as $2p_{3/2} \rightarrow e_g$. This assignment is possible for this octahedral complex with Re having a +4 oxidation state. However, in the present case, although hexacoordinated, the complexes are far from the octahedral symmetry, and therefore the t_{2g}/e_g classification of d-orbitals is not applicable. In addition, the Re^+ atom has a d^6 configuration and therefore the assignment of transitions as $2p_{3/2} \rightarrow t_{2g}$ does not apply as the dπ-orbitals (which end up in the t_{2g} orbitals in octahedral complexes) are filled. Thus, the A and B pre-edge features cannot be localized on the metal atom.

Figure 3 shows the experimental Br K-edge spectra of $[ReBr(CO)_3(bpy)]$ in acetonitrile (MeCN, red) and *N*,*N*-dimethylformamide (DMF, blue). The spectra exhibit a main edge feature (labeled A) at 13.48 keV and an additional one (labeled B) at 13.505 keV. Feature A is markedly different in the two solvents and, in fact, a doublet structure emerges in DMF. The appearance of a solvent effect at the Br K-edge is due to the fact that the Br ligand is directly exposed to the solvent and it senses different local environments more than the Re atom for which no such effect is observed, as it sits at the center of the complex and is thus protected from the solvent.

Time-Resolved XAS. The blue trace in Figure 4 reproduces the XAS of ground-state $[ReBr(CO)_3(bpy)]$ in DMF and the red dots represent the normalized transient Re L_3-edge spectrum (excited minus unexcited absorption) recorded using the high repetition rate scheme.[27] The inset zooms into the pre-edge region. Distinct changes are seen below and above the ground-state absorption edge, whereas weaker ones also appear at higher energies. In particular, there is a clear increase

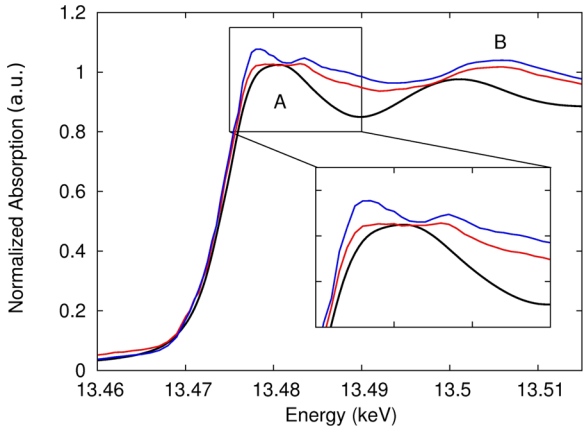

Figure 3. Normalized ground-state Br K-edge X-ray absorption spectrum of $[ReBr(CO)_3(bpy)]$ in MeCN (red) and DMF (blue). The black line is the simulated Br K-edge of $[ReBr(CO)_3(bpy)]$ in the gas phase, calculated using FDMNES. Inset: enlargement of the A feature.

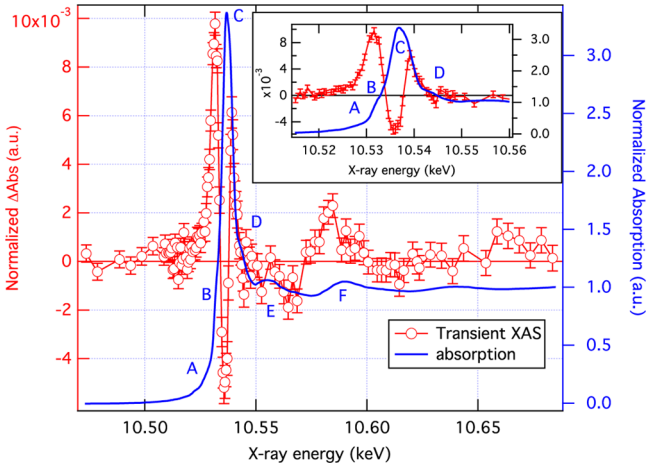

Figure 4. Normalized Re L_3-edge transient XAS signal of a 30 mM solution of $[ReBr(CO)_3(bpy)]$ in DMF (red markers) measured 630 ps after excitation with 355 nm The ground-state XAS is also shown for comparison (blue line) with the features labeled A–F. Inset: zoom into the near-edge region to show the details of the transient XAS. The signal was recorded in fluorescence yield mode (converted to absorption units), at a fluence of 60 mJ/cm^2 and repetition rate of 260 kHz.

in absorption in the pre-edge region at 10.532 keV, suggestive of a transition made possible by the creation of a hole following photoexcitation. In addition, we also observe a decrease in absorption (at 10.536 keV) which, in conjunction with the increase at 10.539 keV corresponds to a ~0.5 eV blue shift of the excited-state absorption edge, as confirmed by comparing the first derivative of the ground-state spectrum with the transient spectrum. Finally, the absorption increase at 10.585 keV, near the ground-state F feature (10.590 keV), points to a shift to lower energies for this EXAFS feature in the excited state. For the molecular structure, such energy shifts suggest an elongation of the bonds, as confirmed below.

Figure 5 shows the Br K-edge XAS of the ground-state complex in DMF (red) and the transient XAS signal (black) measured under conditions identical to those in Figure 4. The latter exhibits an increase in absorption in the pre-edge region at 13.472 keV and a decrease at 13.479 keV. At 13.465 keV,

dx.doi.org/10.1021/jp3106502 | J. Phys. Chem. A 2013, 117, 361–369

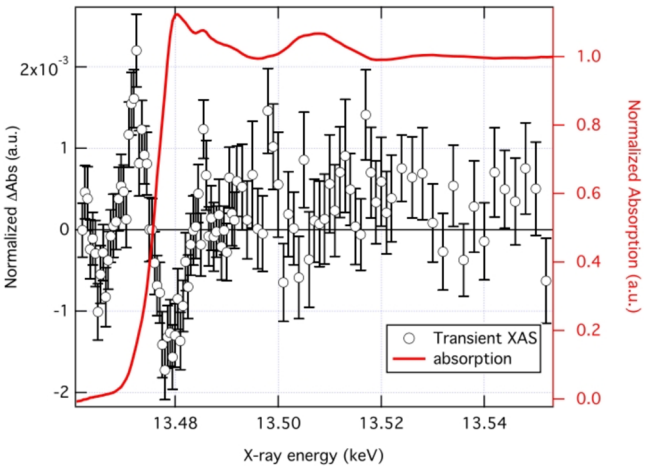

Figure 5. Normalized Br K-edge transient transmission XAS signal of a 30 mM solution of $[ReBr(CO)_3(bpy)]$ in DMF (black markers) measured 630 ps after excitation with 355 nm. The ground-state XAS is also shown for comparison (red line).

there seems to be a weak decrease in absorption, but considering the large error bars, this requires further confirmation. Well above the edge, no clear changes can be seen due to the poor signal-to-noise ratio; however, we note that the experimental data points are on average above the zero difference level. The origin of this vertical offset may be due to a change of atomic background in changing the oxidation state of the atom, in what is known as the atomic X-ray absorption fine structure (AXAFS), due to scattering of the photoelectron from the periphery of the absorbing atom.[28] A similar behavior was reported in the case of photogenerated iodine atoms in aqueous solutions.[12]

In refs 2 and 22 we showed that the emissive ^{3}CT state of all complexes is equilibrated well within 50 ps. This implies that under our present experimental conditions, the system is in the relaxed ^{3}CT state. To confirm that we are actually probing the latter, we recorded the kinetic trace at the maximum of the Re L_3 and Br K-edge pre-edge transient signals, i.e., the features at 10.532 and 13.472 keV, respectively. The time scans are performed under conditions identical to those for the transient XAS measurement but using the liquid jet in place of the flow capillary, and the results are shown in Figure 6. The signals show a pulse-width limited signal rise (<100 ps) followed by a decay of 12.2 ± 0.6 ns and 10.7 ± 1.5 ns for the Re L_3-edge and the Br K-edge, respectively. The agreement between the two demonstrates that these features stem from the same excited species. However, this decay time is shorter than the optical emission decay time (38 ns) in an air-saturated DMF solution, which we determined in the course of this study. This difference is attributed to concentration quenching (triplet−triplet annihilation) due to much higher sample concentration and higher pump fluences used in the X-ray experiment, creating high local concentrations of excited Re complexes. Similar effects were found in the case of $[Ru(bpy)_3]^{2+}$ complexes.[29,30]

Finally, we recorded the Re L_3 transient XAS of 30 mM solutions of $[ReCl(CO)_3(bpy)]$ and $[Re(Etpy)(CO)_3(bpy)]^+$ in DMF. The transient XAS signals of all three samples measured 630 ps (Br, Cl) and 1 ns (Etpy) after excitation are shown in Figure S1, Supporting Information. The general picture is that the normalized transients of the Cl and Etpy complexes are very similar in position, structure, and amplitudes to that of the Br complex. The kinetics of ground-state recovery of the Cl and Etpy complexes in DMF are shown in Figure S2, Supporting Information. The signals for the Cl complex decays in 12.4 ± 0.5 ns, whereas that of the Etpy signal decays in 37 ± 3 ns. Just as for the Br complex, these times deviate from those derived from optical measurements for Cl and Etpy in degassed solution (29 and 230 ns, respectively)[6,31] and likewise, we believe this to be due to triplet−triplet annihilation.

DISCUSSION

Analysis of the Steady-State Spectra. *Re L_3 EXAFS Spectrum.* Starting with the DFT derived geometry for $[ReBr(CO)_3(bpy)]$ (Table 1), we optimize the structure to fit the EXAFS spectrum using the IFEFFIT package.[32] The model includes ten fitting parameters: the amplitude reduction factor (S_0^2), the ionization potential (E_0), ΔR_{Re-C}, ΔR_{Re-N}, ΔR_{Re-Br}, ΔR_{Re-O}, σ_{Re-C}^2, σ_{Re-N}^2, σ_{Re-Br}^2, and σ_{Re-O}^2. Here ΔR_{Re-L} denote the distance changes, with respect to the DFT optimized geometry and σ_{Re-L}^2 represents the uncertainty in the neighbor distance (also called the Debye−Waller factor).

Figure 7a shows the experimental EXAFS spectrum in *k*-space (black) and the best fit (red), whereas Figure 7b shows their corresponding Fourier transform yielding the pseudoradial

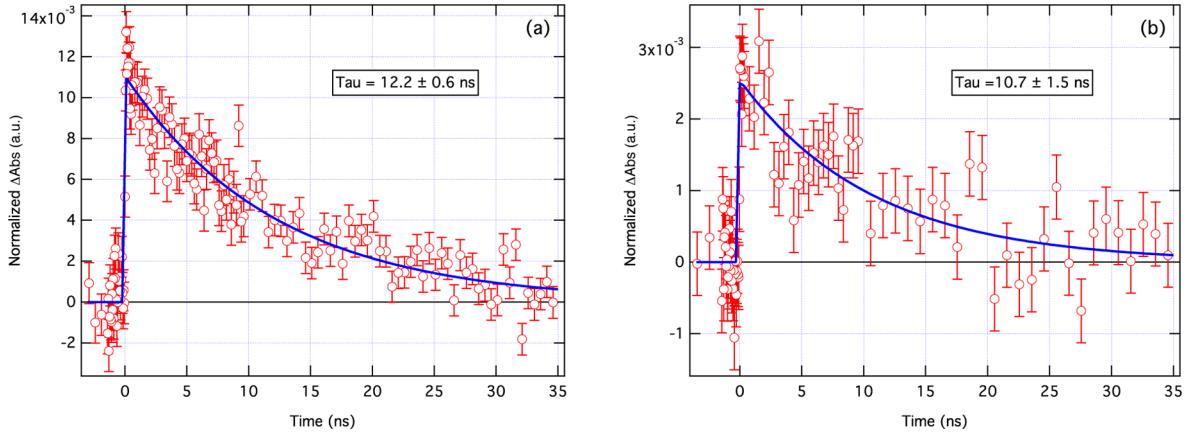

Figure 6. (a) Kinetic trace of the Re L_3-edge transient XAS signal (measured in transmission) at 10.532 keV of $[ReBr(CO)_3(bpy)]$ in DMF. (b) Kinetic trace of the Br K-edge transient XAS signal at 13.472 keV of $[ReBr(CO)_3(bpy)]$ in DMF.

dx.doi.org/10.1021/jp3106502 | J. Phys. Chem. A 2013, 117, 361−369

Table 1. Structural Parameters of the EXAFS Fit, Ground State (GS), and Triplet MLLCT (^{3}CT) State of [ReBr(CO)$_3$(bpy)] from the DFT Optimized Geometry[2,22] [a]

	EXAFS Fit		GS	^{3}CT
	R (Å)	σ^2 (Å^2)	R (Å)	R (Å)
Re−C$_{eq}$	1.91	0.0034	1.92	1.97
Re−C$_{ax}$	1.91	0.0034	1.92	1.96
Re−N	2.18	0.0040	2.20	2.128
Re−Br	2.61	0.0044	2.67	2.52
Re−O$_{eq}$	3.06	0.0028	3.08	3.11
Re−O$_{ax}$	3.06	0.0028	3.08	3.11
C2−C2	1.46		1.46	1.41
	Angle (deg)			
N−Re−N	73.2		73.2	76.7
C$_{eq}$−Re−C$_{eq}$	89.7		89.7	84.1
Br−Re−C$_{ax}$	175.7		175.7	177.5
N−Re−Br	81.3		81.3	89.13

[a]The values for C2−C2 and below are kept fixed during the EXAFS fit.

distribution function. The structural parameters extracted from the fit are summarized in Table 1 and show only small deviations from the DFT optimized geometry. The percentage importance of the scattering path (C_{cw}, Table S2, Supporting Information) from the EXAFS calculation shows that the Re−C−O scattering paths dominate the spectrum demonstrating the role of the focusing effect.[33] Surprisingly, despite its size, the effect of the Br scattering path is small and is due to the fact that it scatters at higher k-values. Such effects have previously been reported for a diplatinum complex[34,35] for which the Pt−Pt scattering pathway contributed only weakly to the overall spectrum. This observation is confirmed in the simulation of the XANES spectrum, discussed in the next section and have recently been rationalized using a wavelet transform study, showing that the limited k-range is the main cause of this insensitivity.[36] Overall we can assign the three peaks of the FT in 7b to the Re−C, Re−N, and Re−O bond distances. The Re−Br peak should appear between the Re−N and Re−O, but as it has little effect on the spectrum, it is not visible.

Re L$_3$ XANES Spectrum. Figure 8 shows a zoom of the pre-edge and the XANES regions. Using the EXAFS optimized structure (Table 1), we simulated the XANES spectrum by means of the MS theory implemented within the FDMNES package.[23] The agreement between the experiment and calculated spectrum is satisfactory but not quantitative. The

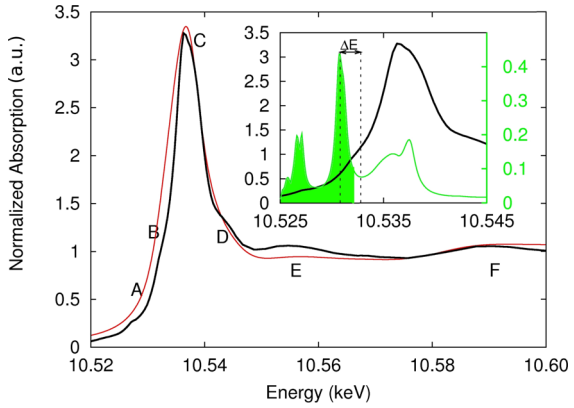

Figure 8. Normalized XANES Re L$_3$-edge of the [ReBr(CO)$_3$(bpy)] complex in DMF (black) and calculated spectrum (red). Inset: zoom of the edge region of the spectrum (black) and the Re d-DOS of states (green line), which has been normalized against the total DOS (corresponds to right axis of the inset). The solid green area represents density, which is below E_F and will therefore play no role in this spectrum. The vertical dotted lines represent the position of the peak of the d-DOS below E_F and the B feature; ΔE is the energy gap between them, which is approximately 2 eV.

inset of Figure 8 shows a zoom of the spectrum close to the white line, the C feature, and also shows the calculated Re d-density of states (d-DOS) normalized against the total DOS, which can be used to extract more details of the nature of the transitions. The calculated Fermi energy (E_F), i.e., the 2p$_{3/2}$ → HOMO gap, is 10.531 keV.

For a detailed assignment of the [ReBr(CO)$_3$(bpy)] spectrum, we first focus on the C band. The L$_{2,3}$-edges of transition metal complexes with an empty or partially occupied metal d-shell exhibit a strong white line arising from the dipole-allowed transitions from the 2p$_{1/2,3/2}$ core orbitals into unoccupied valence d-orbitals.[8,37] For Re$^+$ (5d^6 configuration), the white line transition (C), arises from transitions into d orbitals, as seen from the density of states (DOS) (green line, Figure 8 inset) and due to the oxidation state these must be the empty molecular orbitals with dσ content. This DOS shows two peaks at the energy of the C feature separated by ~2 eV. This originates from a splitting of the dσ orbitals due to the low molecular symmetry and is manifested in the experimental spectrum by the shoulder on the high-energy side of the C band. The d-DOS at lower energy is at or below the HOMO (shaded green area) and it therefore plays no role in the ground-state spectrum.

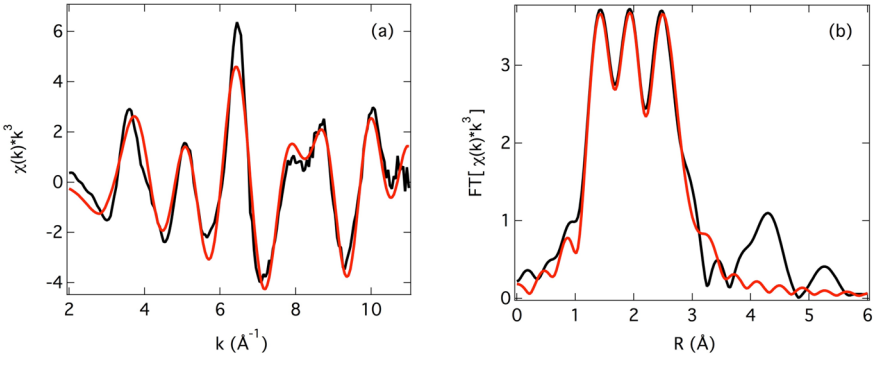

Figure 7. (a) k^3-weighted $\chi(k)$ (black) of [ReBr(CO)$_3$(bpy)] in DMF together with its fit (red). (b) Magnitude of the FT of $k^3\chi(k)$. No phase correction has been applied to the Fourier transform.

dx.doi.org/10.1021/jp3106502 | J. Phys. Chem. A 2013, 117, 361−369

The calculated spectrum shows no clear unoccupied DOS (Figure 8 inset) corresponding to the A and B features. However, the maximum of the largest d-DOS just below the HOMO, corresponding to occupied high-lying molecular orbitals is $\Delta E \sim 2$ eV (Figure 8, inset) lower in energy than the B feature (10.32 keV). This is close to the expected HOMO−LUMO gap,[38] therefore suggesting that the B feature originates from transitions to the lowest-lying unoccupied MO set. Given the previous description of the valence space,[1,2,4,5] (Table S1, Supporting Information) the B band should exhibit a metal-to-ligand character dominated by the CO and bpy ligands and such transitions have frequently been reported in K-edge spectra.[39−41] We rule out a metal-to-halogen transitions because the spectra are rather insensitive to this ligand and the halogen has a fully occupied shell. More detailed investigations are still required to elucidate the origin of the A and B bands, as this is beyond the scope of the present study.

The D, E, and F features, which lie above the ionization potential (IP), are best assigned using a shell-by-shell analysis.[42] This consists in gradually increasing the number of atoms around the rhenium atom, so that the appearance of the resonances can be attributed to specific scattering paths. The simulations are depicted in Figure 9, showing the calculated spectra both with and without the arctangent convolution.[43] The structures used for each calculation are shown aside. In Figure 9b, a cluster consisting of Re and 3 carbon atoms is considered. The resulting spectrum only exhibits structures, which can be associated to the C and F features. This demonstrates that the origin of the C feature is, as expected, primarily a localized Re d-DOS, whereas the F feature is caused by scattering of the C atoms. Upon inclusion of the ligand structure (Figure 9c,d), whereas the F feature is conserved additional details appear: the splitting of the peak corresponding to the C feature, and structures that may be associated with the E feature. In particular, the E and F features become more pronounced upon inclusion of the oxygens (Figure 9c), due to the well-known focusing effect for linear bonds.[33] Indeed, as the number of ligand atoms is increased further (Figure 9d), these resonances are damped due to the symmetry breaking of the molecule.

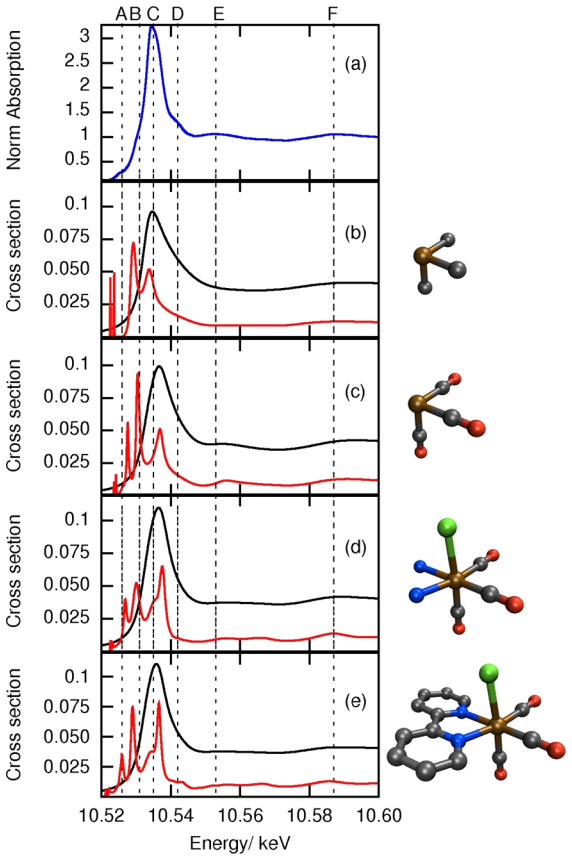

Figure 9. (a) Experimental normalized Re L_3-edge of the [ReBr(CO)$_3$(bpy)] complex in DMF. (b)−(e) Shell by shell simulation of the ligand effect on the cross section calculated using the MS theory, plotted with (black) and without (red) broadening. The structures used are shown on the right-hand side.

Finally, inclusion of the whole bpy ligand (Figure 9e) gives rise to a peak corresponding to the D feature (in the unconvoluted spectrum) and is reminiscent of similar features reported for $[Ru(bpy)_3]^{2+}$.[44] In addition to the calculations presented in Figure 9, we also tested the effect of adding the Br to the Re(CO)$_3$ structure, but no clear difference was observed. As for the EXAFS spectrum, it appears that the XANES spectrum is insensitive to this ligand. In conclusion, the C feature is predominantly due to transitions from $2p_{3/2}$ to a set of molecular orbitals with a 5dσ contribution. The D to F bands are MS structural features, which reflect predominant scattering either at the bpy or at the CO ligands.

Br K-Edge XANES Spectrum. The Br K-edge spectrum of this complex is a challenging problem for MS theory, as the strongly mixed electronic structure means that the constant interstitial potential of the muffin tin (MT) approximation hinders a good description of the spectrum. The FDMNES method[23] offers an alternative way of calculating the spectrum using free-form potentials, but it is computationally intensive due to the size of the molecule and its low symmetry.

The calculated XANES spectrum (Figure 3), based upon the FDMNES method without the solvent and using the molecular structure from the EXAFS fit of Figure 7 shows a rather poor agreement with the experimental spectra. Evidently, the solvent contribution cannot be neglected but, at this point, simulating such effects is prohibitive. Nevertheless, to highlight the differences of the solvent structure around Br, we performed QM/MM MD simulations of the solvent shell structure around the molecule.

Figure 10 shows the integrated radial distribution function (IRDF) of the Br−X distance in both solvents obtained by averaging a 2.5 ps QM/MM MD trajectory. Here, X represents the atom types in the solvent (C, N, and O), which are presented as one data set for each solvent owing to the Z (nuclear mass) $\pm$ 1 sensitivity of XAFS.[45] Figure 10 shows that there are more scatterers within 6 Å in DMF than in MeCN. It is therefore not surprising that the MS features appear different in these two solvents. Ideally, snapshots from these simulations would be used to calculate the XAS spectrum with the surrounding solvent, as was already performed for various solutes in solution.[12,46−49] However, such calculations are, at present, too computationally demanding.

■ ANALYSIS OF THE EXCITED-STATE SPECTRA

Electronic Structure. We will first concentrate on the case of the bromo complex. As suggested in ref 2, photoexcitation of the complex induces a charge transfer from the Re−Br moiety to the bpy ligand. As the electron is transferred to the bpy ligand, a hole is created in the Re-d and Br-p orbitals. In the ground state, Re has 6d electrons, which means that the

dx.doi.org/10.1021/jp3106502 | J. Phys. Chem. A 2013, 117, 361−369

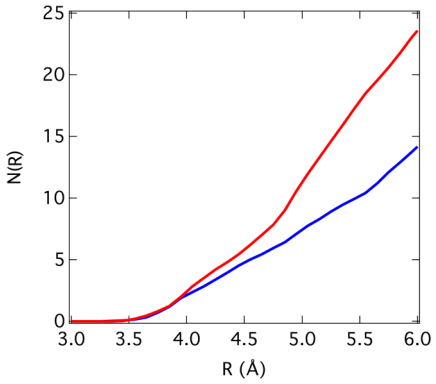

Figure 10. Integrated radial distribution function, $N(R)$, of Br−X in MeCN (blue) and DMF (red) in the vicinity of $[ReBr(CO)_3(bpy)]$. Here, X is the combined integrated radial distribution function for each atomic species (except hydrogen) present in the particular solvent. These have been combined into one data set because the sensitivity of XAS means that atoms which differ by $Z \pm 1$ are indistinguishable.

bonding d_{xy}, d_{xz}, and d_{yz} orbitals are fully occupied. Upon excitation, a hole is created in these orbitals, which can now be accessed from the $2p_{3/2}$ core orbital, causing the appearance of the pre-edge absorption at 10.532 keV in Figure 4. This is similar to what we had reported for the L_3-edge of photoexcited $[Ru(bpy)_3]^{2+}$ [8,50] and $[Pt_2(P_2O_5H_2)_4]^{4-}$.[37]

The ∼+0.5 eV shift of the main band C in the excited-state spectrum is synonymous with the oxidation state of the absorbing atom, which is typically ∼1−2 eV.[8,50,51] In the present case, the smaller shift would appear to confirm the picture of the mixed moiety in which electron density is transferred from both the Re and the Br. However, despite the electronic structural changes between the three complexes, all three transient spectra (Figure S1, Supporting Information) are remarkably similar and these can therefore be used as a lower bound for the sensitivity of the pre-edge region to the electronic structural changes.

At the Br K-edge, a hole also occurs at the 4p orbital as a result of photoexcitation, allowing a transition from the 1s core orbital, which then causes the appearance of the pre-edge feature at 13.473 keV in Figure 5. A similar behavior was recently reported at the L_1-edge due to the 2s−5p transition when iodine ($5p^5$) was generated by abstracting an electron from iodide ($5p^6$) in aqueous solutions.[12] The appearance of the bound−bound core transitions in the pre-edge regions of the Re L_3 and the Br K-edge transitions are the first direct evidence of the MLLCT character of the photoexcitation, which transfers electron density from the metal−halogen moiety to the bpy ligand, as predicted by theoretical calculations.[2,7,22] Obviously, our data are recorded hundreds of picoseconds after excitation, and we cannot conclude as to whether the electron density is simultaneously withdrawn from both atoms. Ultrafast XAS measurements with femtosecond time resolution[12,52] should be able to address this issue. For the X = Cl and Etpy complexes, the similarity of the pre-edge feature in all cases is due to the same reason as in the Br complex, i.e., creation of a hole in the lower bonding d-orbitals by photoinduced transfer of the electron to the bpy ligand.

Molecular Structure. In the following we will determine the structure of the excited complex using both the EXAFS and the XANES regions of the spectrum. To extract excited-state structural parameters, one can generate its spectrum using eq S1, Supporting Information, but the photolysis yield has to be known with precision.[11] It is usually obtained from separate laser-only measurements, but here, this is not possible because the transient absorption spectrum lacks a clear ground-state depletion and is largely dominated by excited-state absorption.[22,53]

Rather, we directly calculate the difference between the ground state and the excited-state EXAFS spectra, which is shown in Figure 11 (left panel), using the DFT optimized molecular structure for both the ground and the excited state of the complex (Table 1) and the excitation yield as an adjustable parameter. Extracting the excited-state model is done using the Artemis code[54] and consists in calculating the excited-state XANES and EXAFS spectrum using the nonstructural parameters (Debye−Waller factors, amplitude reduction factor, E_0) obtained from fitting of the GS spectrum.

The best agreement between the simulation and the experimental EXAFS transient is obtained for a value of the photolysis yield of $f = 2.4\%$ (Figure 11, left panel). This is cross-checked by a fit of the XANES spectra (Figure 11, right panel), for which a similar agreement is observed. This value of f is significantly lower than the calculated one (∼10%), but the calculations do not consider loss processes of the beam,

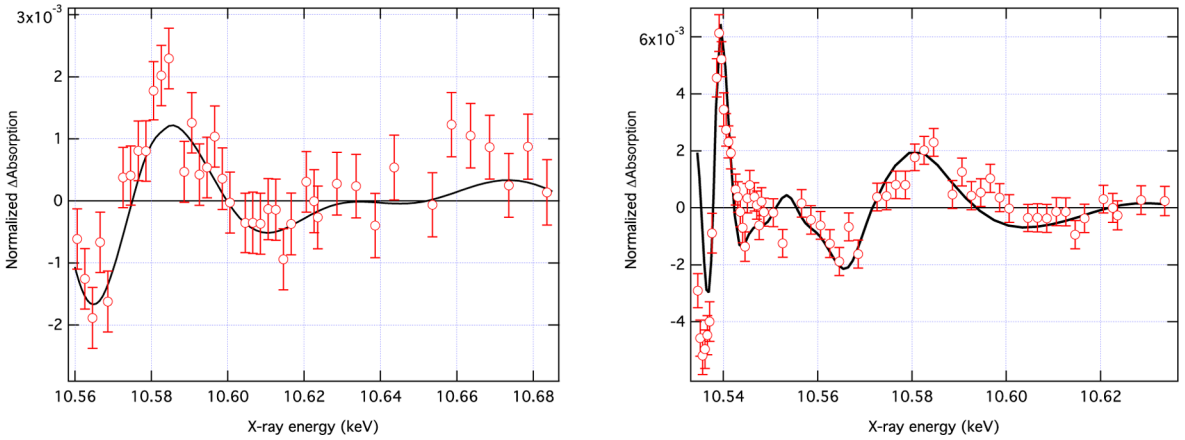

Figure 11. Comparison between the FEFF[21] calculations (black curves) and the experimental transient signal (red markers) in the EXAFS (left) and XANES (right) regions of the Re L_3-edge spectrum of $[ReBr(CO)_3(bpy)]$. In both cases a photolysis yield of 2.4% gives a good agreement for the data of the MHz experiment.

dx.doi.org/10.1021/jp3106502 | J. Phys. Chem. A 2013, 117, 361−369

scattering, etc. In any case, the consistency of the EXAFS and XANES spectra for the same value of f leads us to conclude that the DFT optimized geometries give a good description of the molecular structure and therefore the changes that occur in the ^{3}MLLCT state.

CONCLUSION

We have used static and picosecond X-ray absorption spectroscopy to probe the electronic and geometric structure of ground and excited $[ReX(CO)_3(bpy)]^{n+}$, X = Etpy (n = 1), Cl, or Br (n = 0). The ground-state structural refinement shows that the DFT optimized geometry accurately reproduces the experimental Re L_3-edge. This spectrum is dominated by the Re−C−O scattering paths due to the so-called focusing effect. The Br K-edge spectrum shows a distinct solvent effect, due to the fact that the Br ligand is directly exposed to the environment and is therefore sensitive to the different configurations of the nearby solvent molecules, in contrast to the Re atom that sits at the center of the complex.

In the case of X = Br, the transient spectra at both the Re L_3- and Br K-edges shows the emergence of a pre-edge feature, absent in the ground-state spectrum, which is associated with electron depletion from the HOMO, following photoexcitation. Importantly, these features have the same dynamics and this confirms previous predictions that the low-lying excited states of these complexes involve a charge transfer from both the Re and the ligand X and are, as a consequence best described as metal−ligand-to-ligand-charge-transfer states.

The DFT optimized ground and excited molecular structures allow us to reproduce the experimental difference XANES and EXAFS spectra. In the ground-state structural refinement, we have shown that the Br atom contributes little to the latter. For the excited-state spectrum, although the Re-halogen bond undergoes one of the largest changes, it is still not the major contribution to the photoinduced changes in the EXAFS spectrum, which, as for the ground-state spectrum is the focusing effect, despite the slight elongation of the Re−N and the Re−C bond distances, respectively.

Finally, somewhat surprisingly, the Re L_3-edge spectra of all three complexes (X = Etpy, Cl and Br) demonstrate that the edge and EXAFS regions of the spectrum are rather insensitive to the ligand X. In particular, despite the differing degree of orbital mixing of the complexes, the transient spectra are very similar and therefore this can be used as a lower bound for the sensitivity of the pre-edge region to the electronic structural changes.

ASSOCIATED CONTENT

Supporting Information

Description of the sample preparation, static and picosecond X-ray absorption experiments, simulations, structural parameters, character of the valence molecular orbitals, transient spectra of $[ReX(CO)_3(bpy)]^{n+}$ (X = Etpy, Cl and Br) and time scans of transient features. This material is available free of charge via the Internet at http://pubs.acs.org/.

AUTHOR INFORMATION

Corresponding Author

*E-mail: A.V., a.vlcek@qmul.ac.uk; M.C., majed.chergui@epfl.ch.

Present Addresses

[¶]Chemical Physics, University of Lund, P.O. Box 124, SE-22100 Lund, Sweden.

[#]Arthur Amos Noyes Laboratory, Chemical Physics, Physical Biolology, Center for Ultrafast Science and Technology, Pasadena, CA 91125, USA.

[@]Pacific NW National Laboratory, Chemical and Materials Science Division, Richland, WA 99354 USA.

[△]Max-Planck-Institut fur Chemische Energiekonversion, Stiftstr. 34−36, D-45470 Mulheim an der Ruhr, Germany.

[▽]SwissFEL, Paul-Scherrer-Institut, CH-5232 Villigen, Switzerland.

Notes

The authors declare no competing financial interest.

ACKNOWLEDGMENTS

This work was funded by the Swiss NSF through the NCCR MUST "Molecular ultrafast science and technology" and contracts 200020-127231/1 and 200020-135502. The Czech MSMT grant LD1086, the COST actions D35 and CM0702 and the ESF DYNA Network programme.

REFERENCES

(1) Vlček, A.; Záliš, S. *Coord. Chem. Rev.* **2007**, *251*, 258.
(2) Cannizzo, A.; Blanco-Rodriguez, A.; El-Nahhas, A.; Sebera, J.; Vlček, A.; Záliš, S.; Chergui, M. *J. Am. Chem. Soc.* **2008**, *130*, 8967.
(3) Lo, K. K. W.; Tsang, K. H. K.; Sze, K. S.; Chung, C. K.; Lee, T. K. M.; Hui, W. K.; Li, C. K.; Lau, J. S. Y.; Ng, D. C. N.; Zhu, N. *Coord. Chem. Rev.* **2007**, *251*, 2292−2310.
(4) Kumar, A.; Sun, S.; Lees, A. *Top. Organomet. Chem* **2010**, *29*, 37−71.
(5) Vlček, A. *Top. Organomet. Chem.* **2010**, *29*, 115−158.
(6) Rossenaar, B.; Stufkens, D.; Vlček, A., Jr. *Inorg. Chem.* **1996**, *35*, 2902−2909.
(7) Blanco-Rodriguez, A.; Gabrielsson, A.; Motevalli, M.; Matousek, P.; Towrie, M.; Šebera, J.; Záliš, S.; Vlček, A. *J. Phys. Chem. A* **2005**, *109*, 5016−5025.
(8) Gawelda, W.; Johnson, M.; van de Groot, F.; Abela, R.; Bressler, C.; Chergui, M. *J. Am. Chem. Soc.* **2006**, *128*, 5001−5009.
(9) Chergui, M. *Acta Crystallogr.* **2010**, *66*, 229−239.
(10) Bressler, C.; Chergui, M. *Annu. Rev. Phys. Chem.* **2010**, *61*, 263−282.
(11) Bressler, C.; Abela, R.; Chergui, M. *Z. Kristallogr.* **2008**, *223*, 308−321.
(12) Pham, V.; Penfold, T.; van der Veen, R.; Lima, F.; el Nahhas, A.; Johnson, S.; Beaud, P.; Abela, R.; Bressler, C.; Tavernelli, I.; et al. *J. Am. Chem. Soc.* **2011**, *133*, 12740−12748.
(13) Sarode, P. *J. Chem. Soc., Dalton Trans.* **1979**, 993−995.
(14) Bare, S.; Kelly, S.; Vila, F.; Boldingh, E.; Karapetrova, E.; Kas, I.; Mickelson, G.; Modica, F.; Yang, N.; Rehr, J. *J. Phys. Chem. C* **2011**, *115*, 5740−5755.
(15) Kuzmin, A.; Purans, J.; Dalba, G.; Fornasini, P.; Rocca, F. *J. Phys.-Condens. Matter* **1996**, *8*, 9083.
(16) Sham, T. K.; Heald, S. M. *J. Am. Chem. Soc.* **1983**, *105*, 5142−5143.
(17) Kuzmin, A.; Purans, J.; Benfatto, M.; Natoli, C. *Phys. Rev. B* **1993**, *47*, 2480−2486.
(18) Brown, M.; Peierls, R.; Stern, E. *Phys. Rev. B* **1977**, *15*, 738.
(19) Popov, G.; Greenblatt, M.; Croft, M. *Phys. Rev. B* **2003**, *67*, 024406.
(20) Hilbrig, F.; Michel, C.; Haller, G. *J. Phys. Chem.* **1992**, *96*, 9893−9899.
(21) Rehr, J.; Kas, J.; Prange, M.; Sorini, A.; Takimoto, Y.; Vila, F. *C. R. Phys.* **2009**, *10*, 548.

(22) el Nahhas, A.; Cannizzo, A.; van Mourik, F.; Blanco-Rodriguez, A.; Záliš, S.; Vlček, A.; Chergui, M. *J. Phys. Chem. A* **2010**, *114*, 6361−6369.
(23) Joly, Y. *Phys. Rev. B* **2001**, *63*, 1−10.
(24) Laio, A.; VandeVondele, J.; Rothlisberger, U. *J. Phys. Chem. B* **2002**, *106*, 7300−7307.
(25) Laio, A.; VandeVondele, J.; Rothlisberger, U. *J. Chem. Phys.* **2002**, *116*, 6941−6947.
(26) Rothlisberger, U.; Carloni, P. *Lect. Notes Phys.* **2006**, *704*, 437−466.
(27) Lima, F.; Milne, C.; Amarasinghe, D.; Rittmann-Frank, M.; van der Veen, R.; Reinhard, M.; Pham, V.; Karlsson, S.; Johnson, S.; Grolimund, D.; et al. *Rev. Sci. Instrum.* **2011**, *82*, 063111.
(28) Ramaker, D.; Mojet, B.; Koningsberger, D.; O'Grady, W. *J. Phys.: Condens. Matter.* **1998**, *10*, 8753.
(29) Tarnovsky, A. N.; Gawelda, W.; Johnson, M.; Bressler, C.; Chergui, M. *J. Phys. Chem. B* **2006**, *110*, 26497−26505.
(30) Saes, M. Picosecond X-ray absorption spectroscopy: application to coordination chemistry compounds in solution. *Ph.D. thesis*, EPFL, 2004.
(31) Hino, J.; Della-Ciana, L.; Dressick, W.; Sullivan, B. *Inorg. Chem.* **1992**, *31*, 1072−1080.
(32) Newville, M. *J. Synchrotron Radiat.* **2001**, *8*, 322−324.
(33) Zabinsky, S. I.; Rehr, J. J.; Ankudinov, A.; Albers, R. C. *Phys. Rev. B* **1995**, *52*, 2995.
(34) van der Veen, R. M.; Milne, C. J.; Pham, V. T.; El Nahhas, A.; Weinstein, J. A.; Best, J.; Borca, C. N.; Bressler, C.; Chergui, M. *Chimia* **2008**, *62*, 287−290.
(35) van der Veen, R.; Milne, C.; el Nahhas, A.; Lima, F.; Pham, V.; Best, J.; Weinstein, J.; Borca, C.; Abela, R.; Bressler, C.; et al. *Angew. Chem., Int. Ed. Engl.* **2009**, *48*, 2711−2714.
(36) Penfold, T.; Tavernelli, I.; Milne, C.; Reinhard, M.; El Nahhas, A.; Abela, R.; Rothlisberger, U.; Chergui, M. *J. Chem. Phys.* **2013**, *138*, 014104.
(37) van der Veen, R.; Kas, J.; Milne, C.; Pham, V.; el Nahhas, A.; Lima, F.; Vithanage, D.; Rehr, J.; Abela, R.; Chergui, M. *Phys. Chem. Chem. Phys.* **2010**, *12*, 5551−5561.
(38) Stor, G. J.; Stufkens, D. J. J.; Vernooijs, P.; Baerends, E. J.; Fraanje, J.; Goubitz, K. *Inorg. Chem.* **1995**, *34*, 1588.
(39) Ray, K.; Debeer-George, S.; Solomon, E. I.; Wieghardt, K.; Neese, F. *Chem.—Eur. J.* **2007**, *13*, 2783−2797.
(40) DeBeer-George, S.; Petrenko, T.; Neese, F. *J. Phys. Chem. A* **2008**, *112*, 12936−12943.
(41) Debeer-George, S.; Petrenko, T.; F, N. *Inorg. Chim. Acta* **2008**, *361*, 965−972.
(42) Briois, V.; Sainctavit, P.; Long, G. J.; Grandjean, F. *Inorg. Chem.* **2001**, *40*, 912−918.
(43) Buňau, O.; Joly, Y. *J. Phys.: Condens. Matter.* **2009**, *21*, 345501.
(44) Benfatto, M.; della Longa, S.; Hatada, K.; Hayakawa, K.; Gawelda, W.; Bressler, C.; Chergui, M. *J. Phys. Chem. B* **2006**, *110*, 14035−14039.
(45) Koningsberger, D.; Mojet, B.; Van Dorssen, G.; Ramaker, D. *Top. Catal.* **2000**, *10*, 143−155.
(46) Penfold, T.; Curchod, B.; Tavernelli, I.; Abela, R.; Rothlisberger, U.; Chergui, M. *Phys. Chem. Chem. Phys.* **2012**, *14*, 9444−9450.
(47) Pham, V.; Tavernelli, I.; Milne, C.; van der Veen, R.; D'Angelo, P.; Bressler, C.; Chergui, M. *Chem. Phys.* **2010**, *371*, 24−29.
(48) D'Angelo, P.; Benfatto, M.; Della-Longa, S. *Phys. Rev. B* **2002**, *66*, 064209.
(49) D'Angelo, P.; Migliorati, V.; Guidoni, L. *Inorg. Chem.* **2010**, *49*, 4224−4231.
(50) Saes, M.; Bressler, C.; Abela, R.; Grolimund, D.; Johnson, S.; Heimann, P.; Chergui, M. *Phys. Rev. Lett.* **2003**, *90*, 47403.
(51) de Groot, F.; Hu, Z. W.; Lopez, M. F.; Kaindl, G.; Guillot, F.; Tronc, M. *J. Chem. Phys.* **1994**, *101*, 6570.
(52) Bressler, C.; Milne, C.; Pham, V.; ElNahhas, A.; van der Veen, R.; Gawelda, W.; Johnson, S.; Beaud, P.; Grolimund, D.; Kaiser, M.; et al. *Science* **2009**, *323*, 489−492.
(53) Záliš, S.; Consani, C.; El-Nahhas, A.; Cannizzo, A.; Chergui, M.; Hartl, F.; Vlček, A., Jr. *Inorg. Chim. Acta* **2011**, *374*, 578−585.
(54) Ravel, B.; Newville, M. *J. Synchrotron Radiat.* **2005**, *12*, 537−541.